

## microRNA-143 is associated with the survival of ALDH1<sup>+</sup>CD133<sup>+</sup> osteosarcoma cells and the chemoresistance of osteosarcoma

Jiahui Zhou<sup>1</sup>, Song Wu<sup>1</sup>, Yuxiang Chen<sup>2</sup>, Jingfeng Zhao<sup>2</sup>, Kexiang Zhang<sup>1</sup>, Jianlong Wang<sup>1</sup> and Shijie Chen<sup>1</sup>

<sup>1</sup>Department of Orthopedics, Third Xiangya Hospital, Central South University, Changsha 410013, China; <sup>2</sup>Hepatobiliary and Enteric Surgery Research Center, Xiangya Hospital, Central South University, Changsha 410008, China  
Corresponding author: Song Wu. Email: wusong08@hotmail.com

### Abstract

This study investigated the role of miR-143 in the chemoresistance of osteosarcoma tumor cells and the associated mechanisms. Real-time PCR was used to measure miR-143 levels. Western blot was used to detect protein expression. Cell proliferation was analyzed by MTT assay and Matrigel colony formation assay. Forced miR-143 expression was established by adenoviral vector infection. Cell death was detected by Hoechst33342 staining. Loss of miR-143 expression was observed in osteosarcomas, which correlated with shorter survival of patients with osteosarcomas underlying chemotherapy. In chemoresistant SAOS-2 and U2OS osteosarcomas cells, miR-143 levels were significantly downregulated and accompanied by increases in ATG2B, Bcl-2, and/or LC3-II protein levels, high rate of ALDH1<sup>+</sup>CD133<sup>+</sup> cells, and an increase in Matrigel colony formation ability. H<sub>2</sub>O<sub>2</sub> upregulated p53 and miR-143, but downregulated ATG2B, Bcl-2, and LC3-I expression in U2OS cells (wild-type p53) but not in SAOS-2 (p53-null) cells. Forced miR-143 expression significantly reversed chemoresistance as well as downregulation of ATG2B, LC3-I, and Bcl-2 expression in SAOS-2- and U2OS-resistant cells. Forced miR-143 expression significantly inhibited tumor growth in xenograft SAOS-2-Dox and U2OS-Dox animal models. Loss of miR-143 expression is associated with poor prognosis of patients with osteosarcoma underlying chemotherapy. The chemoresistance of osteosarcoma tumor cells to doxorubicin is associated with the downregulation of miR-143 expression, activation of ALDH1<sup>+</sup>CD133<sup>+</sup> cells, activation of autophagy, and inhibition of cell death. miR-143 may play a crucial role in the chemoresistance of osteosarcoma tumors.

**Keywords:** osteosarcoma, miR-143, autophagy, apoptosis, ALDH1<sup>+</sup>CD133<sup>+</sup> cell

*Experimental Biology and Medicine* 2015; 240: 867–875. DOI: 10.1177/1535370214563893

### Introduction

Osteosarcoma is the most common primary bone malignancy and accounts for over 60% of all malignant bone tumors in children.<sup>1</sup> Over the past several decades, a combination of neoadjuvant chemotherapy, surgery, and adjuvant chemotherapy has led to a dramatic increase in the survival of patients with localized osteosarcoma. The overall five-year survival of osteosarcoma patients with no metastatic disease at diagnosis is 60–70%.<sup>2,3</sup> However, osteosarcoma patients with metastatic or recurrent disease have extremely poor prognosis, with only 20% surviving at 5 years.<sup>4,5</sup> Even though a number of clinical trials have been conducted with increased intensity and refinements in cytotoxic chemotherapy regimens, survival has not been significantly improved for the past 20 years. This disappointing outcome was thought to be associated with locally aggressive growth, early metastatic potential, and frequent acquisition of drug-resistant phenotypes in cancer cells subjected

to chemotherapy. Identifying molecular signaling mechanisms underlying the resistance of osteosarcoma cancer cells to chemotherapy may make way for novel treatment strategies for this disease.

MicroRNA (miRNA) is a class of endogenously expressed, non-coding small RNA with a length of about 17–25 nucleotides. miRNA regulates gene expression at the post-transcriptional level through imperfectly binding to the 3'-untranslated region (3'-UTR) of target mRNA.<sup>6</sup> Current bioinformatics approaches suggest that a single miRNA may regulate anywhere from several hundred to over one thousand genes. In tumor cells, miRNA can function as either an oncogene or a tumor suppressor depending on the specific signal transduction pathways involved. miRNA has been implicated in the regulation of various cellular processes that are often deregulated during tumor development and progression.<sup>6–8</sup> Recent studies have demonstrated that deregulation of miRNA expression is

involved in the invasion, metastasis, angiogenesis, and progression of osteosarcoma.<sup>9</sup> Recently, miR-143 has been reported to be downregulated in some types of cancers. For example, downregulation of miR-143/145 correlated with the lung metastasis of human osteosarcoma cells, while overexpression of miR-143/145 suppressed cell invasion and angiogenesis.<sup>10,11</sup> In addition, increased expression of a panel of tumorsuppressive microRNAs (miRNAs), including miR-34a, miR-143, miR-145, and miR-200b/c that were typically lost in osteosarcoma, was observed during diallyl trisulphide treatment,<sup>12</sup> which suggested that miRNAs may be involved in the chemotherapeutic response of osteosarcoma. However, the role of miRNAs in the chemoresistance of osteosarcoma has not been widely reported.

In this study, we investigated the expression of miR-143 in osteosarcoma tissues and its role in the prognosis of patients with osteosarcomas underlying chemotherapy. We then further investigated the role of miR-143 in the chemoresistance of osteosarcoma cells to doxorubicin *in vitro* and *in vivo*.

## Materials and methods

### Human osteosarcoma tissue samples

The tumor tissues, demographic information, and survival information of 45 patients with primary osteosarcomas were obtained at Xiangya Hospital and Third Xiangya Hospital, Central South University. Surgical resections were subjected to standard clinical and histopathological evaluation using hematoxylin and eosin (H&E) stain. All tumor tissues were excised prior to the initiation of chemotherapy. Chemotherapy regimen included a combination of high-dose doxorubicin and cisplatin or methotrexate, doxorubicin, and cisplatin. Thirteen normal bone samples (femur/tibia) of individuals from similar age groups were obtained through the Department of Orthopedics, Xiangya Hospital and Third Xiangya Hospital. This study was approved by the institutional review board of Central South University.

### Cell culture

Human SAOS-2 and U2OS osteosarcoma cell lines and human hFOB1.19 osteoblast cell lines were obtained from American Type Culture Collection (ATCC, Rockville, MD, USA). Cells were cultured in DMEM (4.5 g/L glucose)/F12 (1:1) medium, supplemented with 10% heat-inactivated FCS (Invitrogen; Carlsbad, CA), at 37°C in a humidified atmosphere of 5% CO<sub>2</sub>.

### Isolation of ALDH1<sup>+</sup>CD133<sup>+</sup> and ALDH1<sup>-</sup>CD133<sup>-</sup> cell subsets

The trypanized SAOS-2 and U2OS cells were suspended at a concentration of  $1 \times 10^6$ /mL in 37°C DMEM/F12K medium. To sort ALDH1<sup>+</sup>CD133<sup>+</sup> and ALDH1<sup>-</sup>CD133<sup>-</sup> cells, each  $10^6$  cells were incubated with FITC-anti-human ALDH1 mAb and APC-anti-human CD133 mAb (BioSS, China) for 1 h in the dark, and then rinsed with  $1 \times$  PBS and incubated with fixation and permeabilization solutions.

ALDH1<sup>+</sup>CD133<sup>+</sup> and ALDH1<sup>-</sup>CD133<sup>-</sup> cells were sorted with MoFlo flow cytometry (Dako, CA, USA). ALDH1<sup>+</sup>CD133<sup>+</sup> and ALDH1<sup>-</sup>CD133<sup>-</sup> subpopulations from SAOS-2 and U2OS cells were re-plated. ALDH1<sup>-</sup>CD133<sup>-</sup> subpopulation was re-plated to establish a doxorubicin resistant cell line of SAOS-2 and U2OS cells. ALDH1<sup>+</sup>CD133<sup>+</sup> subpopulation was directly used for molecular analysis.

### Establishment of doxorubicin-resistant SAOS-2 and U2OS cells

The doxorubicin-resistant SAOS-2 and U2OS cell lines were established by continuously culturing ALDH1<sup>-</sup>CD133<sup>-</sup> SAOS-2 and U2OS cells in medium containing stepwise increases of doxorubicin over a period of nine months. Briefly, SAOS-2 and U2OS (ALDH1<sup>-</sup>CD133<sup>-</sup>) cells were incubated at a beginning concentration of 50 ng/mL of doxorubicin, and then the concentration was escalated stepwise to 1500 ng/mL with medium changes weekly.

### Evaluation of doxorubicin resistance level and MTT assay

MTT (3-[4,5 dimethylthiazol-2-yl]-2,5-diphenyl tetrazolium bromide) was used to measure the IC<sub>50</sub> values of doxorubicin as previously described.<sup>13</sup> Briefly,  $1 \times 10^4$  resistant and non-resistant SAOS-2 and U2OS cells were seeded into 96-well plates. After 24 h, doxorubicin was diluted to a range of concentrations and added to the cells for 72 h. Twenty five microliters of MTT (5 mg/mL) were added to the cells and incubated at 37°C for 4 h. The MTT solution was then removed, and 200  $\mu$ L of isopropanol containing 5% 1 M HCl was added to each well. The optical density was measured at 490 nm. The cells exposed to only culture medium served as experimental control and eight duplicated wells were used for each treatment.

### Matrigel colony assay

Cells were incubated with or without 0.25  $\mu$ M of doxorubicin for 2 h.  $5 \times 10^4$  single cell suspensions were resuspended in a 1:1 mixture of Matrigel (BD Sciences, Franklin Lakes, NJ, USA) to medium and plated on 6-well plates in a limiting dilution. After 15 days of incubation, cells were incubated with 1 mg/mL of iodinitrotetrazolium chloride solution (Sigma-Aldrich, St. Louis, MO, USA), and colonies were counted. Five replicate dishes were plated for each dilution.

### Real-time PCR

Quantitative real-time PCR was used to detect miR-143 expression in cells and tissues. Total RNA from SAOS-2 and U2OS cells and tumor tissues was extracted using Trizol (Invitrogen, Carlsbad, CA, USA) and reverse transcription was performed using One Step PrimeScript<sup>®</sup> miRNA cDNA Synthesis kit. Quantitative PCR reactions were carried out using the SYBR Premix Ex Taq<sup>™</sup> kit (TaKaRa, Japan). Relative quantification (RQ) of miRNA-143 expression was determined by comparative CT method ( $RQ = 2^{-\Delta\Delta CT}$ ) and normalized to U6 level. The miR-143 was amplified using forward

primer: 5'-GGTGCAGTGCTGCATCTCTGGT-3' and reverse primers provided with the kit. U6 was amplified using forward primer: 5'-GCAAGGATGACACGCAAATTC-3' and reverse primers provided with the kit.

### Western blot

The antibodies for p53, Bcl-2, and the peroxidase-labeled secondary antibody were purchased from Cell Signaling Technology (Beverly, MA, USA). The anti-beta actin, anti-ATG2B, anti-LC3-I and LC3-II antibodies were purchased from Sigma-Aldrich (St. Louis, MO, USA). Cells were homogenized and Western blot was performed as previously described.<sup>13</sup> Briefly, 30 µg of total protein was loaded onto a 4–15% SDS-PAGE gel and transferred to PVDF membranes. After blocking with 5% non-fat milk for 1 h, membranes were then incubated with primary antibody overnight at 4°C. After washing with PBS, membranes were incubated with HRP-labeled secondary antibody (1:2000 dilution) for 2 h at room temperature the next day. Immunoreactive proteins were detected using a chemiluminescence reagent (Pierce, Rockford, IL, USA) by following the user manual. To control for loading efficiency, the blots were stripped and re-probed with beta actin antibody.

### Preparation of adenovirus to express miR-143

The short hairpin RNAs expressing miR-143 were cloned into the shuttle vector of an adenovirus packaging system. The expression of the short hairpin was driven by the H1 promoter. Successful cloning was confirmed by sequencing. Preparation and packaging of adenoviruses were performed as previously described.<sup>14</sup> SAOS-2-Dox and U2OS-Dox cells were then transduced at a multiplicity of infection (MOI) of 10. The control plasmid was pSilencer-NC (NC stands for negative control), which is a plasmid with a non-targeting sequence (5'-AATTCTCCG AACGTGTCACGT-3') that replaces the miR-143 sequence.

### Hoechst staining

Cell death induced by AdmiR-143 infection was observed by Hoechst33342 (Calbiochem, San Diego, CA) staining as previously described.<sup>13</sup> Briefly, cells were fixed in methanol/acetic acid (3:1) for 10 min at 4°C, followed by staining with Hoechst33342 (5 µg/mL) for 10 min at room temperature. Cell death was evaluated using a DAPI filter under a fluorescence microscope. Cells that showed clear condensation and small bright nucleus were counted as dead cells. To get a quantitative value, five randomly chosen areas were counted and averaged for each sample.

### Animal experiment

Balb/C nude mice (BALB/c, *nu/nu*) weighing about 20 g were provided by the animal center of Shanghai Biological Science Institution and housed in rooms under standard lighting conditions and temperature. Water and food were provided *ad libitum*. All animal experiments were conducted under an approved protocol from Central South University and performed in accordance with the animal care guidelines of the Chinese Council.

Approximately  $2.5 \times 10^6$  SAOS-2-Dox or U2OS-Dox tumor cells were subcutaneously injected into the right hind limbs of mice. After the tumors grew to 6–7 mm in diameter, mice were randomly divided into four groups: AdNC alone, AdNC+Dox, AdmiR-143 alone, and AdmiR-143+Dox group. Each treatment group consisted of nine animals. Mice in the AdNS and AdNC+Dox group were given AdNC injection ( $1 \times 10^8$  Pfu in 50 µL saline). Mice in AdmiR-143 alone and AdmiR-143+Dox group were intratumorally injected with AdmiR-143 ( $1 \times 10^8$  Pfu in 50 µL of saline). This virus injection was performed once per week for a total of three weeks. Mice in the AdNC+Dox and AdmiR-143+Dox groups were injected with doxorubicin (3 mg/kg in 0.05 mL saline was injected intravenously by tail-vein once a week for a total of three weeks). Animals were sacrificed four weeks after first virus injection. Tumors were excised and tumor weights were recorded.

### Statistical analysis

Data were analyzed using SPSS16.0 (Chicago, IL, USA). The tumor growth data were analyzed by one-way analysis of variance followed by Bonferroni paired *t*-test. The two tailed student's *t*-test was used for analysis of gene expression data. All data are presented as mean ± standard error of the mean. A  $P < 0.05$  was considered statistically significant.

## Results

### Lack of miR-143 expression correlated with poor prognosis

The miR-143 expression in tumor tissues of 45 human primary osteosarcomas and 13 normal bone samples was measured by real-time PCR. The expression of miR-143 was significantly lower in osteosarcomas than in normal bone samples (Figure 1a). We further analyzed the association of miR-143 level with the survival of patients with osteosarcomas after chemotherapy. The patients with above average miR-143 levels survived significantly longer than patients with below average miR-143 levels (Figure 1b).

### miR-143 level correlated with the sensitization of osteosarcomas cells to doxorubicin

Real-time PCR showed that miR-143 levels in SAOS-2 and U2OS cells were significantly lower than that in normal human osteoblasts ( $P < 0.001$ ), while miR-143 level in SAOS-2 was significantly lower than that in U2OS cells ( $P < 0.05$ ) (Figure 2a). SAOS-2 is a p53-null cell line and U2OS cells have wild-type *TP53* gene expression. Western blot detected p53 protein expression in U2OS, but not in SAOS-2 cells (Figure 2b). Low miR-143 expression correlated with high levels of ATG2B and Bcl-2 proteins (Figure 2b). MTT assay showed that U2OS cells were more sensitive to doxorubicin (0.25 µM) than SAOS-2 cells (Figure 2c). Matrigel colony assay showed that 0.5 µM of doxorubicin significantly reduced the colony formation ability of U2OS ( $P < 0.05$ ) cells, but not SAOS-2 cells (Figure 2(d) and (e)).

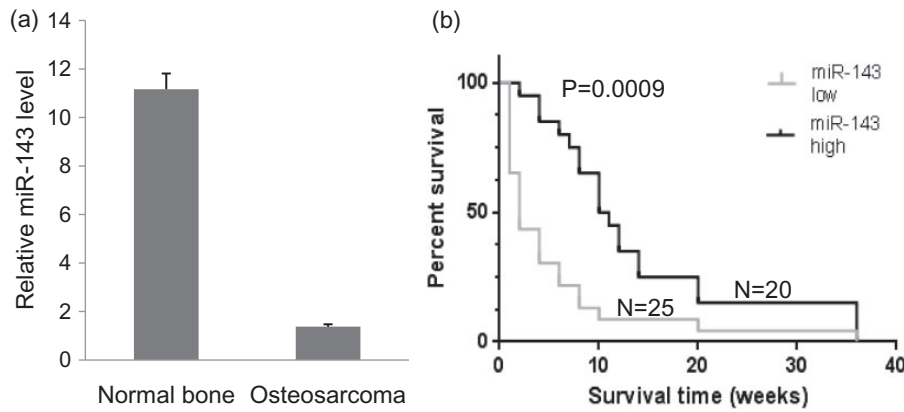


**Figure 1** miR-143 expression and its predictive role in patients with osteosarcoma. (a) Real-time PCR of miR-143 expression in osteosarcoma tumor tissues and normal bone tissues. \* $P < 0.001$ . (b) Survival analysis of patients with osteosarcoma with miR-143 expression higher or lower than the mean. miR-143 low: miR-143 level is lower than the average level of all samples. miR-143 high: miR-143 level is above average miR-143 level

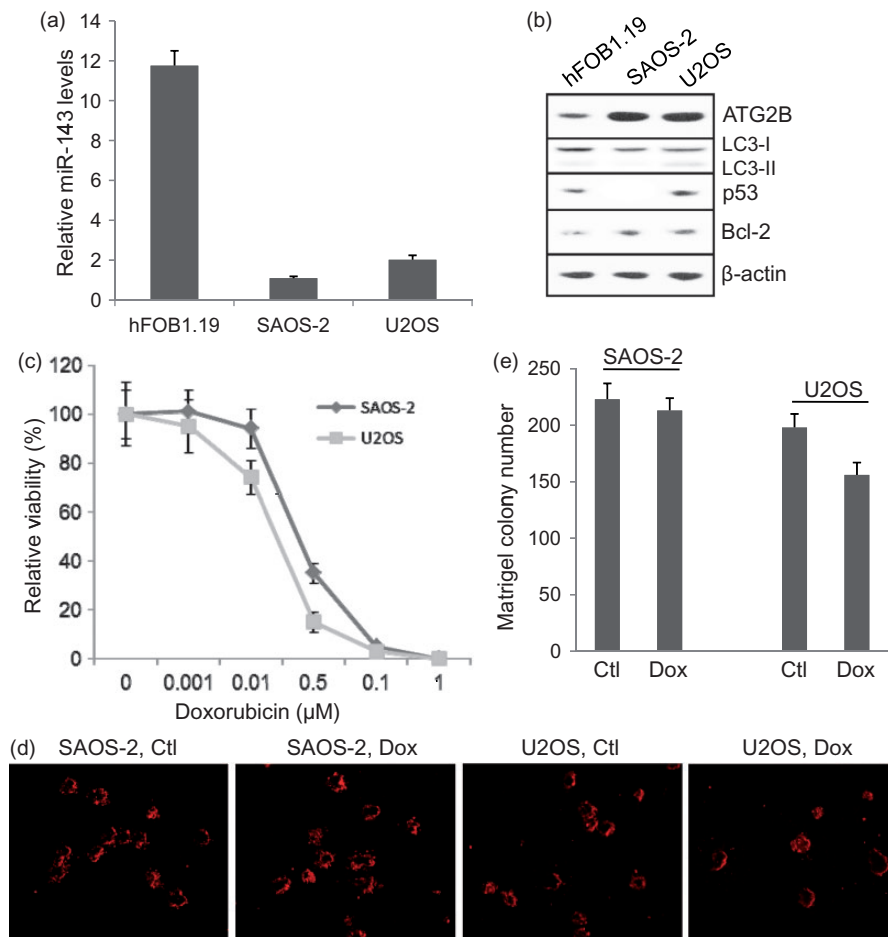


**Figure 2** miR-143 signaling and sensitization to doxorubicin in osteosarcoma cells and normal human osteoblasts. (a) Relative miR-143 expression measured by real-time PCR. (b) Western blot assay of ATG2B, LC3 II/LC3 I, p53 and Bcl-2 protein expression in hFOB1.19, SAOS-2, and U2OS cells. (c) Relative sensitivity of SAOS-2 and U2OS cells to doxorubicin. (d) Representative images of Matrigel colony assay for each group. Ctl: control, Dox: 0.5 mM Doxorubicin treatment. (e) Matrigel colony assay of SAOS-2 and U2OS cells treated with or without 0.5 mM doxorubicin. (A color version of this figure is available in the online journal.)

**miR-143 signaling in chemoresistance and activation of ALDH1<sup>+</sup>CD133<sup>+</sup> cells**

miR-143 levels and associated signaling in non-resistant and resistant SAOS-2 and U2OS cells were compared. miR-143 levels in SAOS-2-Dox cells and U2OS-Dox cells

were significantly downregulated compared to SAOS-2 and U2OS cells ( $P < 0.01$ ,  $P < 0.05$ , respectively) (Figure 3a). Lower miR-143 expression correlated with higher ATG2B, LC3-II, and Bcl-2 protein levels in SAOS-2-Dox cells (Figure 3b). Lower miR-143 expression correlated



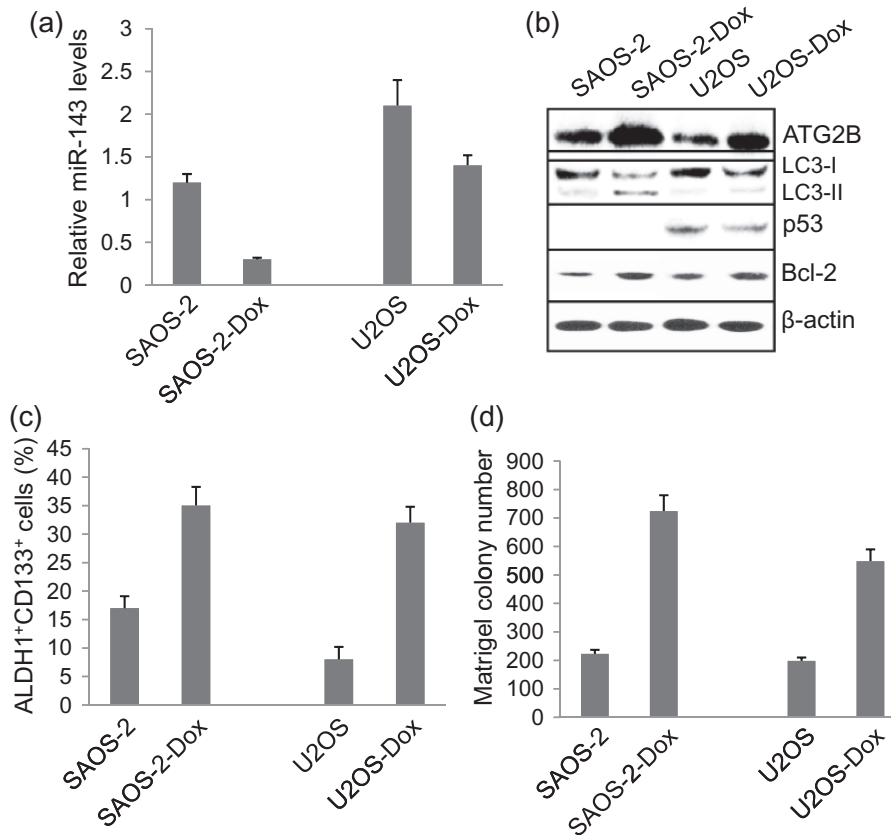


**Figure 3** Role of miR-143 signaling in chemoresistance. (a) miR-143 expression in resistant and non-resistant SAOS-2 and U2OS cells. (b) Western blot assay of ATG2B, LC3 II/LC3 I, p53, and Bcl-2 protein expression. (c) The rate of ALDH1<sup>+</sup>CD133<sup>+</sup> cells isolated from resistant and non-resistant SAOS-2 and U2OS cells. (d) Matrigel colony assay of colony forming ability of resistant and non-resistant SAOS-2 and U2OS cells

with higher ATG2B and Bcl-2 levels in U2OS-Dox cells (Figure 3b). The resistance to doxorubicin was associated with a high rate of ALDH1<sup>+</sup>CD133<sup>+</sup> cells (Figure 3c) and increased Matrigel colony formation ability (Figure 3d) in SAOS-2-Dox and U2OS-Dox cells ( $P < 0.001$ ).

### H<sub>2</sub>O<sub>2</sub> regulates p53 expression and miR-143 signaling in U2OS cells, but not in SAOS-2 cells

Treatment with 0.5 mM of H<sub>2</sub>O<sub>2</sub> significantly reduced cell viability in both U2OS and U2OS-Dox cells (Figure 4(a):  $P < 0.001$ ,  $P < 0.01$ , respectively), but significantly increased miR-143 levels in U2OS and U2OS-Dox cells compared to untreated cells ( $P < 0.001$ ) (Figure 4b). Western blot assay showed that H<sub>2</sub>O<sub>2</sub> treatment increased p53, but decreased ATG2B, LC3-I, and Bcl-2 protein expression in either the U2OS or U2OS-Dox cells (Figure 4c). In contrast, H<sub>2</sub>O<sub>2</sub> treatment significantly reduced cell viability in SAOS-2 cells ( $P < 0.01$ ), but not in SAOS-2-Dox cells (Figure 4d). Also, H<sub>2</sub>O<sub>2</sub> treatment showed no effect on miR-143 mRNA (Figure 4e) or ATG2B, LC3 II/LC3-I, and Bcl-2 protein expression in both SAOS-2 and SAOS-2-Dox cells (Figure 4f).

### Overexpression of miR143 significantly reverses chemoresistance in osteosarcoma cells

SAOS-2-Dox and U2OS-Dox cells were infected with 10 MOI of AdNC control viruses or AdmiR-143 viruses for

48 h and were then subjected to MTT assay and Hoechst33342 staining. AdmiR-143 infection significantly decreased cell viability in both SAOS-2-Dox and U2OS-Dox cells ( $P < 0.001$ ) (Figure 5a) and increased cell death ( $P < 0.001$ ) (Figure 5b) compared to AdNC infection. Matrigel colony formation assay showed that AdmiR-143 infection significantly decreased the colony formation ability in both SAOS-2-Dox and U2OS-Dox cells (Figure 5(c),  $P < 0.001$ ). Western blot showed that AdmiR-143 infection significantly decreased the levels of ATG2B, LC3-I, and Bcl-2 in SAOS-2-Dox and U2OS-Dox cells (Figure 5d).

### Overexpression of miR-143 significantly inhibits tumor growth in xenograft animal model

SAOS-2-Dox and U2OS-Dox tumor cells were inoculated subcutaneously to establish the xenograft animal osteosarcoma models. After the tumors grew to 6–7 mm in diameter, mice were given AdNC alone, AdNC + Dox, AdmiR-143 alone, or AdmiR-143 + Dox injections. AdmiR-143 alone and AdmiR-143 plus doxorubicin injection significantly inhibited tumor growth in xenograft SAOS-2-Dox animal model ( $P < 0.01$  and  $P < 0.001$ ) compared to AdNC and AdNC plus doxorubicin injection (Figure 6a). AdmiR-143 plus doxorubicin injection was more effective than AdmiR-143 injection alone in inhibiting tumor growth ( $P < 0.05$ ) (Figure 6a). Similar results were obtained in U2OS-Dox xenograft animal model (Figure 6b).

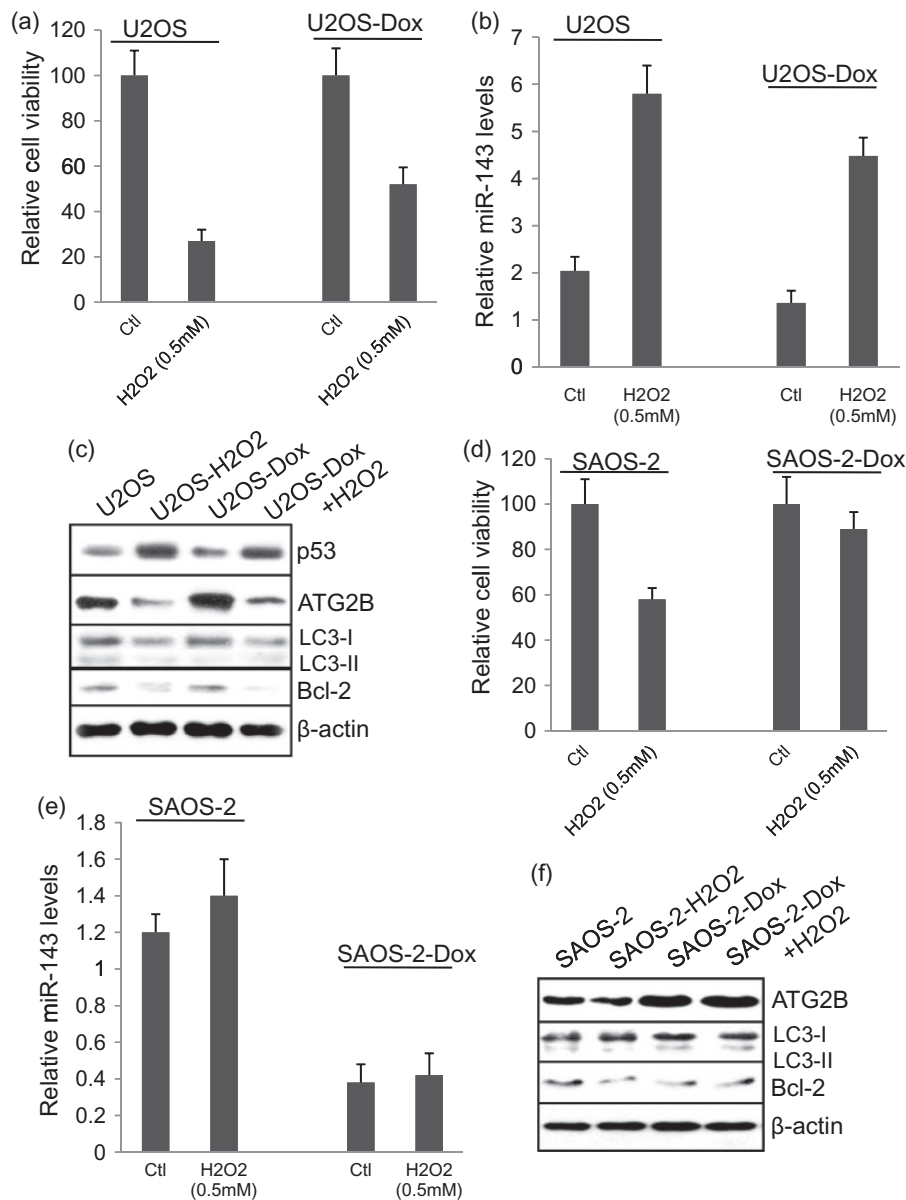


**Figure 4** Role of H<sub>2</sub>O<sub>2</sub> on miR-143 signaling and cell survival. (a) MTT assay of cell viability in U2OS and U2OS-Dox cells treated with or without 0.5 mM H<sub>2</sub>O<sub>2</sub>. (b) Real-time PCR of miR-143 levels in U2OS and U2OS-Dox cells treated with or without 0.5 mM H<sub>2</sub>O<sub>2</sub>. (c) Western blot assay of ATG2B, LC3 II/LC3 I, p53, and Bcl-2 protein expression in U2OS and U2OS-Dox cells treated with or without 0.5 mM H<sub>2</sub>O<sub>2</sub>. (d) MTT assay of cell viability in SAOS-2 and SAOS-2-Dox cells treated with or without 0.5 mM H<sub>2</sub>O<sub>2</sub>. (e) Real-time PCR of miR-143 levels in SAOS-2 and SAOS-2-Dox cells treated with and without 0.5 mM H<sub>2</sub>O<sub>2</sub>. (f) Western blot assay of ATG2B, LC3 II/LC3 I, p53, and Bcl-2 protein expression in SAOS-2 and SAOS-2-Dox cells treated with or without 0.5 mM H<sub>2</sub>O<sub>2</sub>.

## Discussion

Although downregulation of miR-143 expression has been widely observed in various tumor cells and has been found to correlate with invasion, angiogenesis, and lung metastasis of human osteosarcoma cells, its roles in chemoresistance and in predicting the prognosis of patients with osteosarcoma has not been reported. In this study, we first demonstrated that downregulation of miR-143 expression correlated with poor prognosis of patients with osteosarcoma underlying chemotherapy. Interestingly, we found that H<sub>2</sub>O<sub>2</sub> stimulates p53 expression, which is accompanied by upregulation of miR-143 expression and downregulation of ATG2B, LC3II, and Bcl-2 expression, suggesting a signal

regulation of p53-miR143-autophagy/apoptosis. Chemoresistance was found to be associated with the downregulation of miR-143 expression and activation of ALDH1<sup>+</sup>CD133<sup>+</sup> osteosarcoma cells. Our study suggests that miR-143 plays a crucial role in tumor growth and sensitization of osteosarcoma cells to chemotherapy.

In this study, we demonstrated that H<sub>2</sub>O<sub>2</sub> significantly upregulated p53 protein and miR-143 mRNA expression in U2OS osteosarcoma cells expressing wild-type p53 gene. In contrast, H<sub>2</sub>O<sub>2</sub> did not increase miR-143 expression in p53-null SAOS-2 cells. Importantly, the forced expression of miR-143 can reverse the chemoresistance in SAOS-2-Dox- and U2OS-Dox-resistant cells. Also, forced expression of miR-143 significantly inhibited tumor growth in xenograft

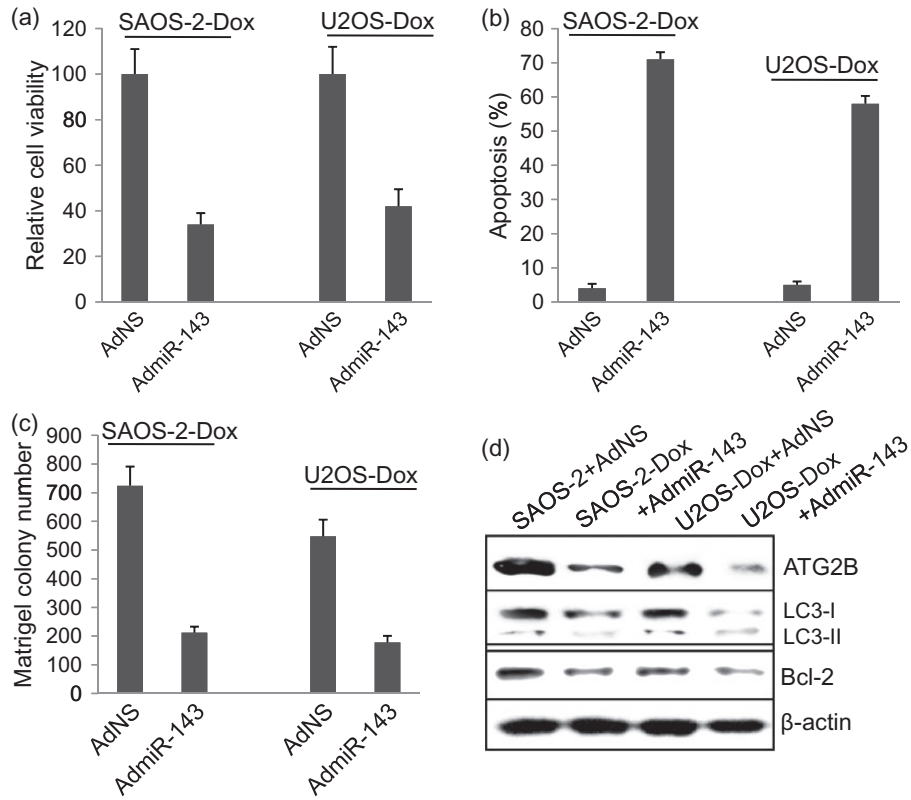


**Figure 5** The role of miR-143 overexpression on osteosarcoma tumor cell survival. (a) Overexpression of miR-143 delivered by adenoviruses significantly reduced cell viability in SAOS-2-Dox and U2OS-Dox cells. (b) Overexpression of miR-143 significantly induced cell apoptosis in SAOS-2-Dox and U2OS-Dox cells. (c) Overexpression of miR-143 significantly inhibited colony forming in SAOS-2-Dox and U2OS-Dox cells. (d) Western blot assay of ATG2B, LC3 I/LC3 II, and Bcl-2 protein expression in SAOS-2-Dox and U2OS-Dox cells infected with AdmiR-143

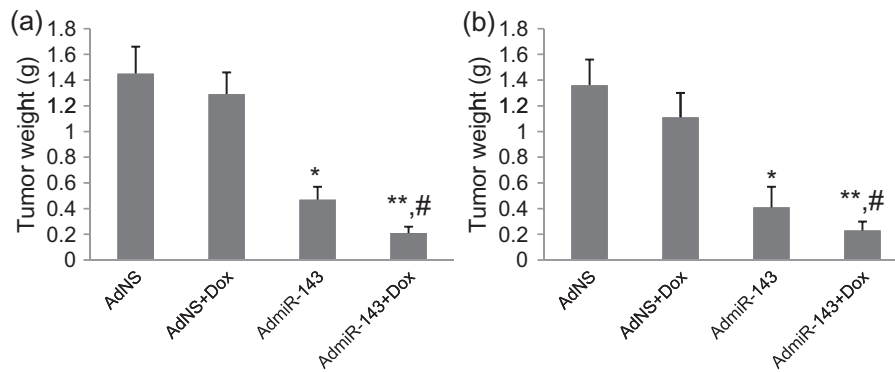


**Figure 6** Tumor growth in xenograft animal models. Xenograft osteosarcoma animal models were established by inoculation of SAOS-2-Dox and U2OS-Dox tumor cells and given AdNS alone, AdNS + Dox, AdmiR-143 alone, and AdmiR-143 + Dox injections. Tumors were excised and weighted. (a) Tumor weights of SAOS-2-Dox xenograft tumors. (b) Tumor weights of U2OS-Dox xenograft tumors. \* $P < 0.001$ , \*\* $P < 0.0001$  vs. AdNS group, # $P < 0.05$  vs. AdmiR-143 group.  $N = 9$

SAOS-2-Dox and U2OS-Dox models. A previous study demonstrated that p53 enhances the post-transcriptional maturation of several miRNAs with growth-suppressive functions in response to DNA damage, including miR-16, miR-143, and miR-145.<sup>15</sup> H<sub>2</sub>O<sub>2</sub> is a DNA damage agent, which has been widely revealed to dose-dependently stimulate p53 expression in tumor cells.<sup>16</sup> Therefore, this observation suggests that miR-143 may be regulated by p53, but may not be directly regulated by H<sub>2</sub>O<sub>2</sub>.

A novel finding in this study is that the chemoresistance to doxorubicin of osteosarcoma cells is associated with the activation of ALDH1<sup>+</sup>CD133<sup>+</sup> positive cells. In this study, the chemoresistant osteosarcoma cells derived from ALDH1<sup>-</sup>CD133<sup>-</sup> SAOS-2 and U2OS cells exhibited significantly higher rate of ALDH1<sup>+</sup>CD133<sup>+</sup> cells compared to that in non-resistant SAOS-2 and U2OS cells. Also, the SAOS-2-Dox and U2OS-Dox cells showed a significant increase in Matrigel colony formation ability. This collectively suggests that ALDH1<sup>+</sup>CD133<sup>+</sup> cells are associated

with chemoresistance in osteosarcoma cells. Furthermore, the activation of ALDH1<sup>+</sup>CD133<sup>+</sup> cells was accompanied by the downregulation of miR-143 expression. In addition, forced expression of miR-143 significantly lowered colony formation ability *in vitro* and inhibited tumor growth *in vivo*. Therefore, our study suggests that miR-143 is a tumor suppressor, which may inhibit the activation of ALDH1<sup>+</sup>CD133<sup>+</sup> cells in osteosarcoma and their subsequent involvement in chemosensitivity.

The second novel finding is that the activation of ALDH1<sup>+</sup>CD133<sup>+</sup> osteosarcoma cells is associated with the activation of autophagy. Autophagy is a physiological mechanism that eliminates toxic wastes or damaged cellular components in response to stress. Recent studies demonstrated that the activation of autophagy and inhibition of apoptosis is involved in the survival of stem cells.<sup>17,18</sup> In this study, we demonstrated that the expression of ATG2B and LC3 II was significantly higher in doxorubicin-resistant SAOS-2 and U2OS cells than in non-resistant cells. Moreover, H<sub>2</sub>O<sub>2</sub> treatment upregulated miR-143 expression and downregulated ATG2B and LC3 II expression in osteosarcoma cells expressing wild-type p53. Forced expression of miR-143 also obviously lowered ATG2B and LC3 II protein levels in p53-null osteosarcoma cells and osteosarcoma cells expressing wild-type p53. During autophagosome formation, microtubule-associated protein light chain 3 I (LC3-I) is conjugated to phosphatidylamine to form LC3-phosphatidylamine (LC3-II). The production of LC3-II is an essential process in the formation of the autophagosome.<sup>19,20</sup> Mammalian ATG2B protein is also essential for autophagosome formation.<sup>21</sup> Therefore, our study clearly suggested that miR-143 regulates autophagy in ALDH1<sup>+</sup>CD133<sup>+</sup> osteosarcoma cells, which is involved in the chemoresistance of osteosarcoma cells.

A number of studies have reported that autophagy is activated in cancer cells in response to various anticancer therapies. The activated autophagy can kill apoptosis-resistant tumor cells.<sup>22</sup> However, a recent study revealed that activation of autophagy results in inhibition of apoptosis.<sup>22</sup> Autophagy signaling usually shares the same pathway with apoptosis. In this study, H<sub>2</sub>O<sub>2</sub> treatment significantly induced cell death in both the U2OS resistant and non-resistant cells accompanied by downregulation of ATG2B and LC3-I expression and upregulation of miR-143 expression. Similarly, overexpression of miR-143 induced cell death in both resistant and non-resistant SAOS-2 and U2OS cells, which was also accompanied by downregulation of ATG2B and LC3-I expression. Bcl-2 has previously been demonstrated to be a direct target of miR-143.<sup>23</sup> Therefore, autophagy and cell death are regulated in the same way by miR-143 in osteosarcoma cells. The balance between autophagy and cell death plays a key role in chemoresistance and growth of osteosarcoma cells.

In conclusion, our study demonstrated first that miR-143 may be involved in the chemoresistance of osteosarcoma cells through controlling the autophagy and activation of ALDH1<sup>+</sup>CD133<sup>+</sup> osteosarcoma cells. This study highlighted the value of miR-143 as a potential target for reversing chemoresistance in osteosarcoma patients.

**Authors' contributions:** All authors participated in the design, interpretation of the studies and analysis of the data and review of the manuscript; JZho, JZha, KZ, JW, and SC conducted the experiments, and SW and YC wrote the manuscript.

#### ACKNOWLEDGEMENT

We acknowledge the financial support of the National Hi-tech Program (863 Project) of China (No. 2007AA021804, 2007AA021809).

#### REFERENCES

1. Link MP. Osteosarcoma in adolescents and young adults: new developments and controversies. Commentary on the use of presurgical chemotherapy. *Cancer Treat Res* 1993;**62**:383-5
2. Bacci G, Ferrari S, Bertoni F, Ruggieri P, Picci P, Longhi A, Casadei R, Fabbri N, Forni C, Versari M, Campanacci M. Long-term outcome for patients with nonmetastatic osteosarcoma of the extremity treated at the istituto ortopedico rizzoli according to the istitutoortopedico rizzoli/osteosarcoma-2 protocol: an updated report. *J Clin Oncol* 2000;**18**:4016-27
3. Rytting M, Pearson P, Raymond AK, Ayala A, Murray J, Yasko AW, Johnson M, Jaffe N. Osteosarcoma in preadolescent patients. *Clin Orthop Relat Res* 2000;**373**:39-50
4. Wu PK, Chen WM, Chen CF, Lee OK, Haung CK, Chen TH. Primary osteogenic sarcoma with pulmonary metastasis: clinical results and prognostic factors in 91 patients. *Jpn J Clin Oncol* 2009;**39**:514-22
5. Petrilli AS, de Camargo B, Filho VO, Bruniera P, Brunetto AL, Jesus-Garcia R, Camargo OP, Pena W, Péricles P, Davi A, Prospero JD, Alves MT, Oliveira CR, Macedo CR, Mendes WL, Almeida MT, Borsato ML, dos Santos TM, Ortega J, Consentino E, Brazilian Osteosarcoma Treatment Group Studies III and IV. Brazilian Osteosarcoma Treatment Group Studies III and IV. Results of the Brazilian Osteosarcoma Treatment Group Studies III and IV: prognostic factors and impact on survival. *J Clin Oncol* 2006;**24**:1161-8
6. Bartel DP. MicroRNAs: genomics, biogenesis, mechanism, and function. *Cell* 2004;**116**:281-97
7. Osaki M, Takeshita F, Ochiya T. MicroRNAs as biomarkers and therapeutic drugs in human cancer. *Biomarkers* 2008;**13**:658-70
8. Profumo V, Gandellini P. MicroRNAs: cobblestones on the road to cancer metastasis. *Crit Rev Oncog* 2013;**18**:341-55
9. Liang W, Gao B, Fu P, Xu S, Qian Y, Fu Q. The miRNAs in the pathogenesis of osteosarcoma. *Front Biosci (Landmark Ed)* 2013;**18**:788-94
10. Fan L, Wu Q, Xing X, Wei Y, Shao Z. MicroRNA-145 targets vascular endothelial growth factor and inhibits invasion and metastasis of osteosarcoma cells. *Acta Biochim Biophys Sin (Shanghai)* 2012;**44**:407-14
11. Osaki M, Takeshita F, Sugimoto Y, Kosaka N, Yamamoto Y, Yoshioka Y, Kobayashi E, Yamada T, Kawai A, Inoue T, Ito H, Oshimura M, Ochiya T. MicroRNA-143 regulates human osteosarcoma metastasis by regulating matrix metalloproteinase-13 expression. *Mol Ther* 2011;**19**:1123-30
12. Li Y, Zhang J, Zhang L, Si M, Yin H, Li J. Diallyl trisulfide inhibits proliferation, invasion and angiogenesis of osteosarcoma cells by switching on suppressor microRNAs and inactivating of Notch-1 signaling. *Carcinogenesis* 2013;**34**:1601-10
13. Zhang X, Huang Q, Yang Z, Li Y, Li CY. GW112, a novel antiapoptotic protein that promotes tumor growth. *Cancer Res* 2004;**64**:2474-81
14. Wang H, Wei F, Zhang J, Wang F, Li H, Chen X, Xie K, Wang Y, Li C, Huang Q. A novel immunocompetent murine tumor model for the evaluation of RCAd-enhanced R2Ad transduction efficacy. *Tumour Biol* 2012;**33**:1245-53
15. Suzuki HI, Yamagata K, Sugimoto K, Iwamoto T, Kato S, Miyazono K. Modulation of microRNA processing by p53. *Nature* 2009;**460**:529-33



16. Jiang MC, Liang HJ, Liao CF, Lu FJ. Methyl methanesulfonate and hydrogen peroxide differentially regulate p53 accumulation in hepatoblastoma cells. *Toxicol Lett* 1999;**106**:201–8
17. Lara-Padilla E, Caceres-Cortes JR. On the nature of the tumor-initiating cell. *Curr Stem Cell Res Ther* 2012;**7**:26–35
18. Wu S, Wang X, Chen J, Chen Y. Autophagy of cancer stem cells is involved with chemoresistance of colon cancer cells. *Biochem Biophys Res Commun* 2013;**434**:898–903
19. Ogata M, Hino S, Saito A, Morikawa K, Kondo S, Kanemoto S, Murakami T, Taniguchi M, Tanii I, Yoshinaga K, Shiosaka S, Hammarback JA, Urano F, Imaizumi K. Autophagy is activated for cell survival after endoplasmic reticulum stress. *Mol Cell Biol* 2006;**26**:9220–31
20. Chaachouay H, Ohneseit P, Toulany M, Kehlbach R, Multhoff G, Rodemann HP. Autophagy contributes to resistance of tumor cells to ionizing radiation. *Radiother Oncol* 2011;**99**:287–92
21. Lin HM, Tseng HC, Wang CJ, Chyau CC, Liao KK, Peng PL, Chou FP. Induction of autophagy and apoptosis by the extract of *Solanum nigrum* Linn in HepG2 cells. *J Agric Food Chem* 2007;**55**:3620–8
22. Warr MR, Binnewies M, Flach J, Reynaud D, Garg T, Malhotra R, Debnath J, Passequé E. FOXO3A directs a protective autophagy program in haematopoietic stem cells. *Nature* 2013;**494**:323–7
23. Liu L, Yu X, Guo X, Tian Z, Su M, Long Y, Huang C, Zhou F, Liu M, Wu X, Wang X. miR-143 is downregulated in cervical cancer and promotes apoptosis and inhibits tumor formation by targeting Bcl-2. *Mol Med Rep* 2012;**5**:753–60

(Received April 17, 2014, Accepted August 27, 2014)